

# Highly stable and reliable capacitive strain sensor for wearable electronics based on anti-dry hydrogel electrode

Jiaoya Huang<sup>a,b</sup>, Runhui Zhou<sup>b</sup>, Ziyu Chen<sup>a</sup>, Yushu Wang<sup>a</sup>, Zemin Li<sup>b</sup>, Xiaoming Mo<sup>a</sup>,  
Naiwei Gao<sup>b,\*\*\*</sup>, Jiang He<sup>b,\*\*</sup>, Caofeng Pan<sup>a,b,c,\*</sup>

<sup>a</sup> Center on Nanoenergy Research, School of Physical Science and Technology, Guangxi University, Nanning, Guangxi, 530004, PR China

<sup>b</sup> CAS Center for Excellence in Nanoscience, Beijing Key Laboratory of Micro-nano Energy and Sensor, Beijing Institute of Nanoenergy and Nanosystems, Chinese Academy of Sciences, Beijing, 101400, PR China

<sup>c</sup> School of Nanoscience and Engineering, University of Chinese Academy of Sciences, Beijing, 100049, PR China

## ARTICLE INFO

### Keywords:

Wearable electronics  
Capacitive strain sensor  
Water-retaining ionic hydrogels  
Long-term stability  
Human motion detection  
Human-machine interaction

## ABSTRACT

Hydrogel-based capacitive strain sensors have been rapidly developed benefiting from their robust structure, excellent flexibility, and high linearity. However, the existing capacitive strain sensors usually suffer from the water evaporation of hydrogel electrodes, leading to poor long-term stability. In this work, a dry-resistant hydrogel electrode with 250  $\mu\text{m}$  thickness was prepared on the dielectric elastomer by a simple and versatile template method through the synergistic water-retention effect of glycerin and LiCl, which can maintain high mechanical stability in a dry environment with relative humidity of 10% RH. The fabricated capacitive strain sensor can be stored in a normal environment for 45 days and can continuously operate under the environment with relative humidity of 20% RH for 40 h (over 10,000 cycles). Most importantly, the capacitive strain sensor possessed ultra-high linearity ( $R^2 > 0.998$ ), good uniformity ( $>93.56\%$ ), and robustness at different humidity. With these favorable advantages, the sensor was successfully applied as a highly reliable wearable sensing system for human motion detection and human-machine interaction in real-time.

## 1. Introduction

Flexible strain sensors are paid more attention due to their enormous potential in the development of the Tactile Internet (TI) [1–4], such as robot control [5,6], motion detection [7,8], human-machine interaction [9,10], and electronic skin [11–15]. Hydrogels have been the competitive electrode candidates for the fabrication of strain sensors due to their skin-like mechanical properties, outstanding stretchability, good biocompatibility, electrical conductivity, and low cost [16–21]. Many works have been devoted to realizing hydrogel-based capacitive strain sensors with excellent sensing performance. For example, Zhang and coworkers fabricated a capacitive strain sensor based on MXene/PVA hydrogel electrodes, which showed good stretchability, high linearity as well as small hysteresis [22]. Mo and colleagues developed a highly stable and durable strain sensor based on the Zn-alginate/PAM hydrogel conductor that could survive being run over by a catastrophic vehicle [23]. However, due to the inevitable evaporation of water from the

hydrogel, the hydrogel-based sensors are susceptible to failure in mechanical or electrical properties after a period of use [24–26], especially under low relative humidity conditions, which is highly detrimental to real-life applications of hydrogel-based sensors.

To improve the water-loss resistance of hydrogels, one of effective strategies is to introduce hygroscopic salts (e.g. LiCl, CaCl<sub>2</sub>, etc.) or organic solvents (e.g. glycerin, ethylene glycol) into the hydrogels [27–32]. Hygroscopic salts dissociate in the water of the hydrogel to form hydrated ions, thus reducing the saturated vapor pressure of the hydrogel [31,33]. Sui and coworkers demonstrated a poly (sulfobetaine-coacrylic acid hydrogel enriched with LiCl that can be stored in an ambient environment (temperature of 25 °C, relative humidity of 54% RH) for 1 week almost without water loss [31]. Similarly, organic solvents tend to form strong hydrogen bonds with water molecules to inhibit the evaporation of water [30,34]. For instance, Sun and colleagues exhibited an organohydrogel based on polyacrylamide, montmorillonite, and carbon nanotube, soaked in glycerin to partially replace

\* Corresponding author. Center on Nanoenergy Research, School of Physical Science and Technology, Guangxi University, Nanning, Guangxi, 530004, PR China.

\*\* Corresponding author.

\*\*\* Corresponding author.

E-mail addresses: [nwgao@szu.edu.cn](mailto:nwgao@szu.edu.cn) (N. Gao), [hejiang@binn.cas.cn](mailto:hejiang@binn.cas.cn) (J. He), [cspan@binn.cas.cn](mailto:cspan@binn.cas.cn) (C. Pan).

the water in the hydrogel, which possessed good stability after 30 days under a normal environment [29]. In principle, such water-retaining hydrogels can be ideal candidates to improve the stability of hydrogel-based capacitive sensors. However, current water-retaining hydrogels are not yet able to meet the requirements of long-term stable capacitive sensors. The design of capacitors with water-loss resistance requires a combination of water-retaining hydrogels and stable interface design. It is limited by the above difficulties that few studies have been devoted to fabricating such a capacitive sensor that is resistant to water loss over time.

Herein, we proposed a highly stable and reliable capacitive strain sensor based on water-retaining hydrogel electrodes, which were prepared by a facile and effective template method and the synergistic water-retention effect of glycerin and LiCl. In the optimized hydrogel system, sodium hyaluronate (SH) and polyacrylamide (PAM) built up the polymer chain backbones, while glycerin and Li<sup>+</sup> were both used to lock the inner water based on hydrogen bonds. As a result, the water-retaining hydrogel with 250 μm thickness can remain stretchable after 24 h in the environment with relative humidity of 10% RH. The anti-dry performance of our hydrogel and other published moisturizing gels were also carefully compared, as shown in Table S1. The fabricated sensor was capable of excellent mechanical durability for 40 h (over 10,000 cycles) under a dry environment with relative humidity of about 20%

RH. Besides, the sensor can also ensure long-term stable performance under a normal environment for up to 45 days, mainly benefiting from the intrinsic stability of the hydrogel electrodes. Inspired by reliable sensing performances, the sensor can be applied to monitor human motion and control the robot in real time, demonstrating its great potential in practical application.

## 2. Results and discussion

### 2.1. Synthesis of stable sodium hyaluronate/polyacrylamide/glycerin/LiCl hydrogel (SPGLH)

To enhance the long-term stability of the sodium hyaluronate/polyacrylamide hydrogel (SPH), as illustrated in Fig. 1a, we added glycerin and LiCl into the pre-gel solution of SPH to lock free water molecules to form SPGLH. In such a system, SH and PAM served as the backbone of the hydrogel, providing a substantial number of hydroxyl groups and amide group. The Li<sup>+</sup>, produced by the hydrolysis of LiCl, formed hydrated ions with water molecules [27,31,35], enabling the physical entanglement of SH and PAM. Meanwhile, the introduction of glycerin contributed to enhancing the interaction of glycerin with water molecules and polymer chains through hydrogen bonds [29,34]. Consequently, the content of free water was diminished thereby

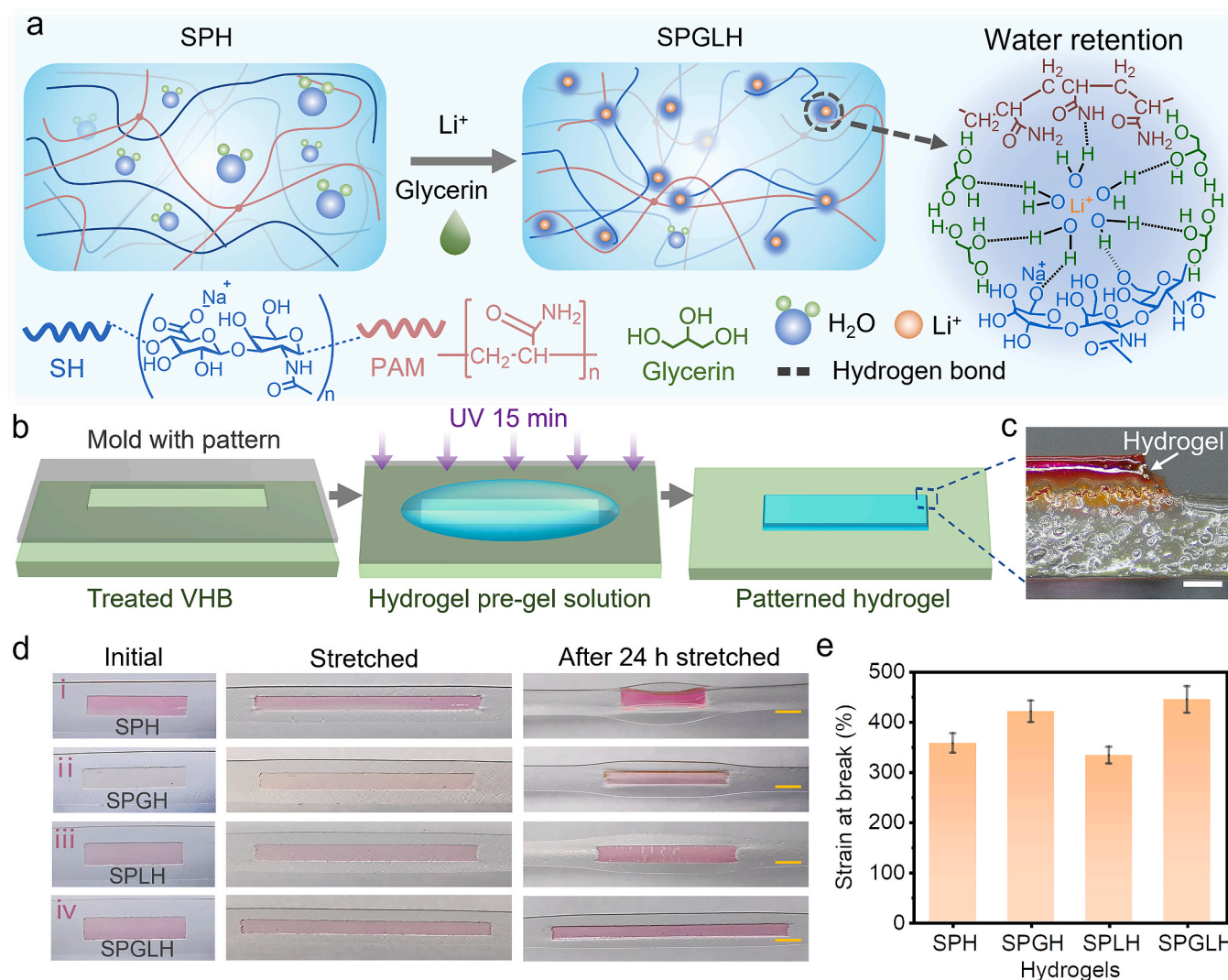


**Fig. 1.** The design and fabrication of SPGLH. (a) The design principle for improving water retention of the hydrogel. (b) The fabrication process of the hydrogel on the dielectric. (c) The cross-section image of colored SPGLH bonding with VHB. Scale bar: 250 μm. (d) Comparison of the anti-dry capacity of SPH, SPGH, SPLH, and SPGLH. Hydrogels were colored by rhodamine. Scale bar: 0.5 cm. (e) The stretchability of SPH, SPGH, SPLH, and SPGLH.

improving the water retention capacity of SPH.

To ensure the uniformity of hydrogel electrodes, a facile and versatile manufacturing method was employed. The fabrication process was shown in Fig. 1b. Firstly, VHB was treated with 10 wt% benzophenone in ethanol and then the anti-sticking PET film with a hollow pattern, which served as the mold, was placed on VHB. Subsequently, the pre-gel solution was poured onto the PET mold and covered with sheet glass. After ultraviolet irradiation for 15 min, removing the PET film and sheet glass, SPGLH was successfully photocured on the VHB surface. Fig. 1c presented a cross-sectional image of SPGLH and VHB, in which the thickness of the hydrogel was approximately 250  $\mu\text{m}$ . As mentioned above, the formation of the SPGLH can be confirmed by the emergence of the SPH. Here, Fourier transform infrared spectrometer (FTIR) and Raman spectroscopy were conducted to characterize the structure of the SPH. The FTIR data in Fig. S1 demonstrated that two peaks of SPH corresponding to C=O and NH<sub>2</sub> were similar to the acrylamide (AM) monomer rather than VHB [36]. Figure. S2 showed that the Raman signal of SPH became weaker in the C=C peak position and stronger in the C-H peak position, indicating SPH was successfully formed on the VHB surface [37]. Besides, the shapes of hydrogels depend on the mold, which is beneficial to uniform the sizes of hydrogel electrodes for capacitive devices later. Fig. S3 showed several patterns of SPGLH photocured by different molds. SPGLH were robustly bonded with VHB without slippage or separation even in stretched states, which exhibited interfacial toughness of 72.23 J/m<sup>2</sup> through the 90° peeling test (Fig. S4). This can be attributed to the grafting or entanglement effect of the light-generating benzophenone ketyl radical on the polymer networks between hydrogels and VHB [38].

Both the water-retention capacity and intrinsic stretchability of hydrogels are important for stable hydrogel-based strain sensors. To study the effects of glycerin and LiCl on dehydration resistance and stretchability, we prepared four different hydrogels, including SPH, sodium hyaluronate/polyacrylamide/glycerin hydrogel (SPGH), sodium hyaluronate/polyacrylamide/LiCl hydrogel (SPLH), and SPGLH on the VHB surface in our fabrication method. As shown in Fig. 1d, these hydrogels with the same size (20 mm × 6 mm × 250  $\mu\text{m}$ ) were placed in the dry condition with a temperature of 18 °C and relative humidity of 10% RH. Initially, all samples were able to be stretched to 150%. Whereas after 24 h, only SPGLH retained its stretchability and the other three samples had been dried out and failed in stretchability, in which SPGLH contained 13.8 wt% glycerin and 16.5 wt% LiCl. To test the environmental tolerance of the hydrogels, the four hydrogels were exposed to a dry environment with temperature of 25 °C and relative humidity of 10% RH for 122 h in Fig. S5a. The weight-time curves of four samples dropped significantly in the previous 14 h, due to the evaporation of free water from hydrogels, and then the residual weight of four samples tended to stabilize. As shown in Fig. S5b, the relative weight of SPGLH remained at 56.7% after 72 h, higher than the other three samples, confirming excellent anti-dry performance, which was attributed to the synergistic water-retention effect of glycerin and LiCl. Meanwhile, the stretchability of SPGLH and SPGH was superior to that of SPH and SPLH in Fig. 1e and Fig. S6, where the average strain of SPGLH before fracture was 445% (Fig. S7). To further quantify the effects of glycerol and LiCl on hydrogels, we prepared hydrogels with different contents of glycerol and LiCl, respectively. As evident from Figs. S8a and S8b, both glycerin and LiCl contributed to improving the water-retention capacity of hydrogels. Nevertheless, the linear-fitting slope of data points in Fig. S8c (0.34) and Fig. S8d (1.18) indicated that LiCl had a greater effect on the dehydration resistance of hydrogels compared to glycerin. Fig. S9 indicated that glycerin facilitated the stretchability of hydrogels compared to LiCl, owing to additional hydrogen bonding [34]. Therefore, we enhanced the anti-dry ability and stretchability of the hydrogel by introducing glycerin and LiCl in this work. Furthermore, the use of LiCl contributed to the conductivity of SPGLH (Fig. S10).

## 2.2. Stable performance of the sensor based on hydrogels

To investigate the influences of stable interfaces and anti-dry hydrogels on devices, we prepared hydrogel-based capacitive strain sensors without encapsulation. Fig. 2a exhibited the structure and working mechanism of the capacitive strain sensor, where stretchable hydrogels were used as electrodes and VHB acted as the dielectric layer due to its intrinsic stretchability and relatively high dielectric constant [39,40]. For stretchable parallel-plate capacitors, the capacitance signal is related to the geometric deformation [41,42]. As shown in Fig. S11, stable interfaces enabled high linearity and stability of hydrogel-based capacitive strain sensors (details in Supplementary Note 1). Furthermore, the anti-dry hydrogel electrode played a vital role in the long-term stability of hydrogel-based devices. Fig. 2b exhibited that the SPH sensor and the SPGLH sensor were both exposed in a dry environment with 11% RH and then were stretched to 100% before and after 1 h. As shown in Fig. 2c, the performance of the SPH sensor dramatically failed after 1 h, because SPH became stiff and lost elasticity due to the loss of the water. In contrast, SPGLH remained stretchable so that the performance of the SPGLH sensor slightly declined (Fig. 2d). These results indicate that stable interfaces and the drying-resistant hydrogel are essential to improving the stability of hydrogel-based capacitive strain sensors.

## 2.3. Sensing characterization of the sensor

Encouraged by the stable performance of the SPGLH strain sensor, we further optimized the sensor construction and characterized the key sensing properties. To protect hydrogel from slow dehydration, the sensors were sealed by elastomers, as shown in Fig. 3a, where a commercial silica-based glue was used to ensure strong bonding between the encapsulation and the dielectric. In Fig. 3b, the SPGLH sensor exhibited ultrahigh linearity ( $R^2 > 0.998$ ) and negligible hysteresis in the range of 190% strain. By contrast, the SPH sensor displayed poor linearity ( $R^2 = 0.962$ ) and significant hysteresis at a small range of 140% strain because the water in the hydrogel inevitably evaporated even after encapsulation [33]. It was further indicated that enhancing the water retention capacity of the hydrogel was important for the high performance of strain sensors. The SPGLH sensor was used to characterize transient responses at strain levels increasing from 20% to 140% with a ramping rate of 10 mm/s. As shown in Fig. 3c, the sensing response of the SPGLH sensor was extremely stable and showed free overshooting behavior under constant static loading, which was a common problem for resistive strain sensors [43,44]. Furthermore, our sensors were capable of high uniformity by enabling standardization of the dimensions of hydrogel electrodes. Fig. 3d showed that six samples present ultra-high linearity and similar amplitudes in the 150% strain range (Fig. 3d), in which the mean variance of these sensors only 6.44% at 150% strain, demonstrating excellent reproducibility (>93.56%), which was beneficial for large-scale applications without individual calibration before usage.

In addition to great performances of linearity, stretchability, and uniformity, the SPGLH sensor also exhibited satisfactory reliability during operation. It is well known that hydrogels containing hygroscopic salts are susceptible to swelling or de-swelling in response to the variation of ambient humidity [33]. To investigate the effect of humidity on the performance of the device, we placed the sensor in the chamber with a temperature of 20 °C and different humidity for 3 h and then tested its electrical response in sequence. As shown in Fig. 3e, the performances of the SPGLH sensor remained almost consistent at different relative humidity levels, indicating its potential in real-life applications. Besides, the sensing performance of the SPGLH sensor maintained for over 45 days under a normal environment in Fig. 3f. Satisfactorily, the SPGLH sensor can endure dynamic deformation continuously for about 40 h at 50% strain under a dry environment with relative humidity of 20% RH and insignificant change in its response signal was observed (lower panels, Fig. 3g, and Fig. S12). In contrast, the signal of the SPH

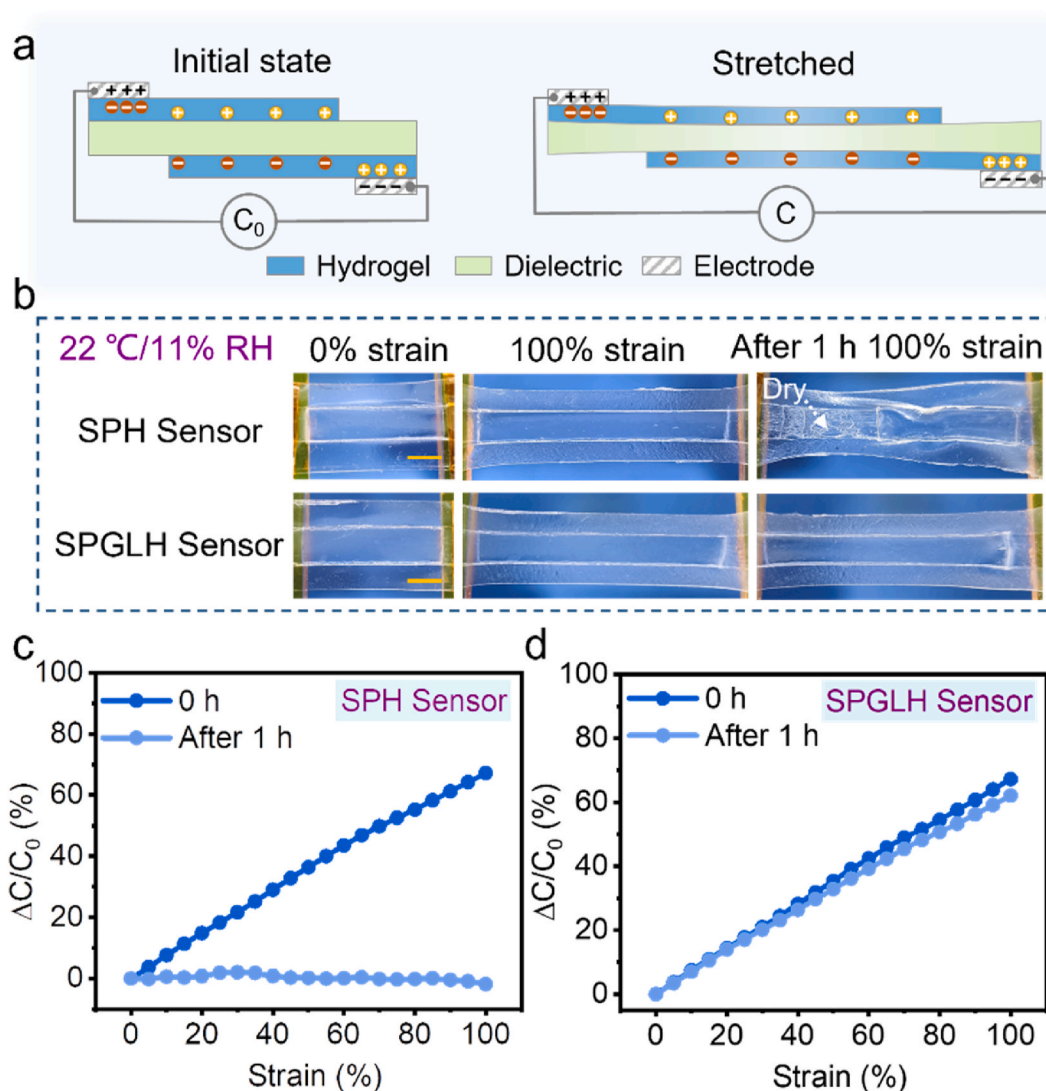


**Fig. 2.** The effect of the water-retention capacity of hydrogels on the performance of strain sensors. (a) The schematic and principle of capacitive strain sensor. (b) Comparison of the water-retention capacity of the SPH sensor and the SPGLH sensor. Scale bar: 0.5 cm. (c) The relatively capacitive change of the SPH sensor in the range of 100% strain before and after 1 h. (d) The relatively capacitive change of the SPGLH sensor in the range of 100% strain before and after 1 h.

sensor was extremely unstable and failed rapidly relatively short period of 6 h (upper panels, Fig. 3g), which was attributed to the gradual drying and hardening of SPH during operation (insets in Fig. 3g). These results indicate that the preparation of the anti-dry hydrogel electrodes is an effective solution to improve long-term stability and reliability of hydrogel-based capacitive strain sensors.

#### 2.4. SPGLH sensor for human motion detection

Owing to stable sensing properties, the SPGLH sensor can be used to monitor human movement in real-life applications. The sensor was attached to human joints by adhesive strips and its response signals were measured by an LCR meter. As shown in Fig. 4a, the sensor was capable of detecting finger bending angles of 0°, 30°, 60°, and 90°. The dynamic bending tests were also conducted in Fig. 4b. The amplitude and frequency of the signal response can reflect the intensity and frequency of the bending motion, respectively. The sensor can also work well in salt water, demonstrating its good resistance to sweat and water (Fig. 4c). Besides, continuous bending deformations of the wrist, elbow, and knee of humans can be detected (Fig. 4d–f). These results indicated that the sensor was capable of detecting of daily activity of human limbs.

#### 2.5. SPGLH sensor for human-machine interaction in real-time

To demonstrate the potential of hydrogel strain sensors in wearable electronics, the sensors were assembled on a wearable glove to realize human-machine interaction in real-time. As shown in Fig. 5a, we constructed the human-machine interaction system, where the response signals of capacitive strain sensors can be converted into pulse waves by multi-harmonic oscillators with NE555 timer and then processed by Arduino to achieve controlling machine hand. The SPH sensor and SPGLH sensor were both used to control the movement of the machine hand in a normal environment with relative humidity of 20% RH, respectively. Fig. 5b showed that both sensors performed normally at the beginning of the operation. However, after 1 day, the SPH sensor failed because its hydrogel electrodes dried out. In contrast, the SPGLH sensor maintained working effectively, indicating its excellent reliability in practical application. Subsequently, five SPGLH sensors were integrated into a wearable glove, which could detect the movement of each finger individually and accurately (Fig. 5c). Based on this wearable sensing system, each finger of the robot was controlled by a human hand synchronously (Supplementary movie and Fig. 5d), demonstrating great potential in performing risky tasks for industrial factories.

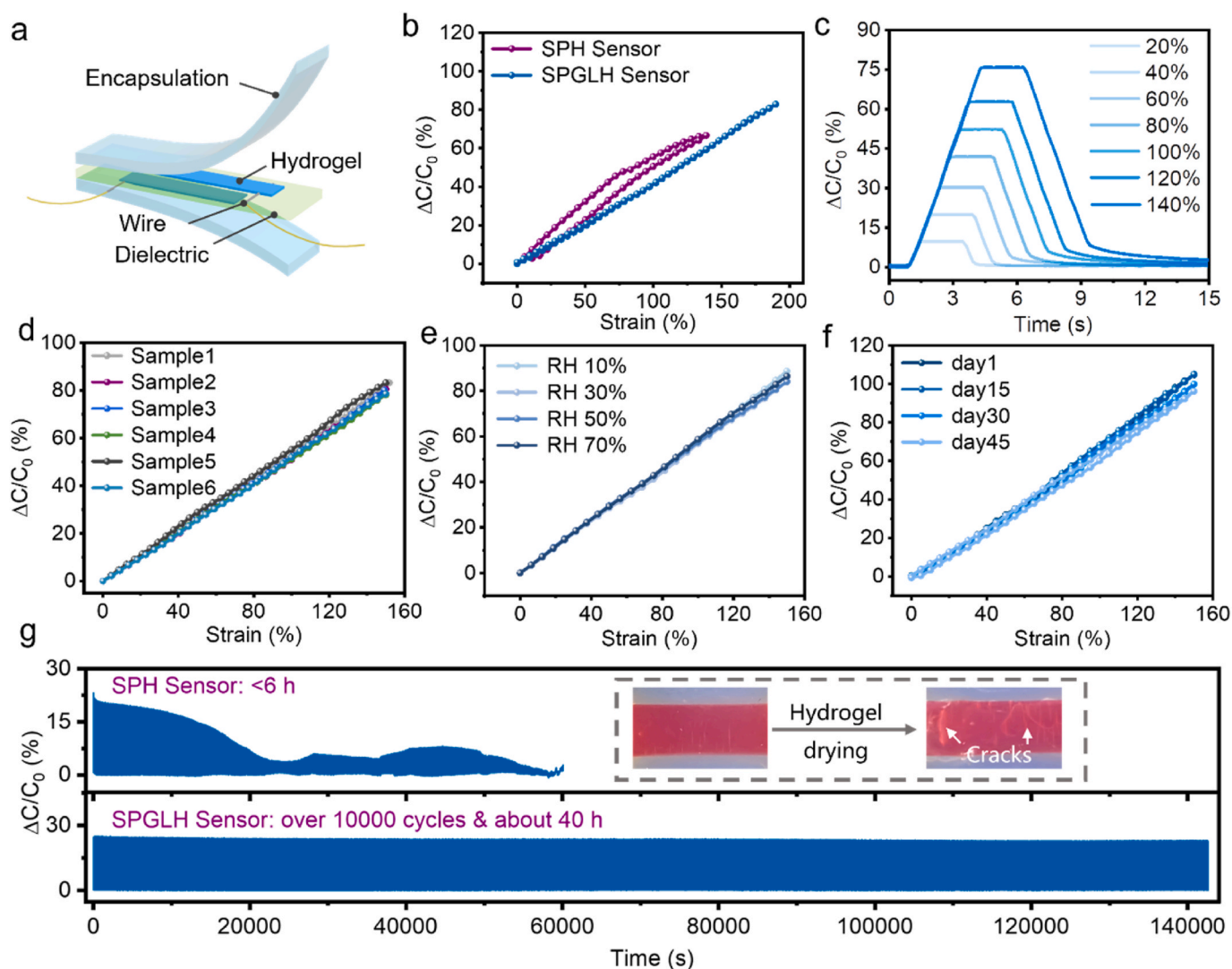


**Fig. 3.** Sensing characterization and signal stability of strain sensors. (a) Schematic of capacitive strain sensor encapsulated by the elastomer. (b) Strain sensing response of the SPH sensor and the SPGLH sensor under stretching and releasing. (c) The relative capacitance change of the SPGLH sensor under different applied strain levels from 20% to 140%. (d) The device-to-device uniformity of the SPGLH sensor in the 150% strain range. (e) The stability of the SPGLH sensor in conditions with a temperature of 20 °C and different relative humidity. (f) The long-term stability of the SPGLH sensor within 45 days. (g) The mechanical stability of the SPH sensor (upper panels) and the SPGLH sensor (lower panels) under a dry environment. Insets of the SPH sensor drying out.

### 3. Conclusion

In summary, we presented a capacitive strain sensor based on a water-retaining hydrogel, demonstrating highly stable and reliable sensing performance even under a dry environment. Owing to the synergistic water-retention effect of glycerin and LiCl, SPGLH with 250  $\mu\text{m}$  thickness remained stretchable for over 24 h under a dry condition with relative humidity of 10% RH. As a result, the fabricated strain sensors based on SPGLH could be stored over 45 days in a normal environment or operated continuously for 40 h (over 10,000 cycles) in a dry environment with relative humidity of 20% RH. Furthermore, the SPGLH sensor also possessed ultra-high linearity ( $R^2 > 0.998$ ), good uniformity ( $>93.56\%$ ), and robustness to different humidity levels. Motivated by these good properties, the SPGLH sensor exhibited high reliability in applications of detecting daily human movements and human-machine interaction, paving the way for long-term stable sensing of hydrogel-based capacitive strain sensors.

### 4. Experimental methods

#### 4.1. Materials

All chemical reagents were used in this work without further purification. SH powder, which was purchased from Shanxi Carryherb Bio Co., Ltd, and AM (99%, Aladdin) were both used for hydrogel polymer networks. LiCl (99%, Innochem) was used as conductive and hygroscopic salts. Glycerin (99%, Aladdin) was used for dehydration resistance. N, N-methylenebisacrylamide (MBAA, 99%, Aladdin) and polyethylene glycol diacrylate (PEGDA, Aladdin) both served as cross-linkers, and 2-Hydroxy-4'-(2-hydroxyethoxy)-2-methylpropiophenone (Irgacure 2959, Aldrich 410896) was used as the photoinitiator. VHB (4905, 3M) was used as a dielectric elastomer. Benzophenone (99.5%, Aladdin) was dispersed in ethanol as the VHB surface treatment reagent. Ecoflex (00-50, Smooth-On) was used as the encapsulation elastomer.

#### 4.2. The fabrication of SPGLH pro-gel solution

SH powder was dissolved in deionized water to form a 2.5 wt.%

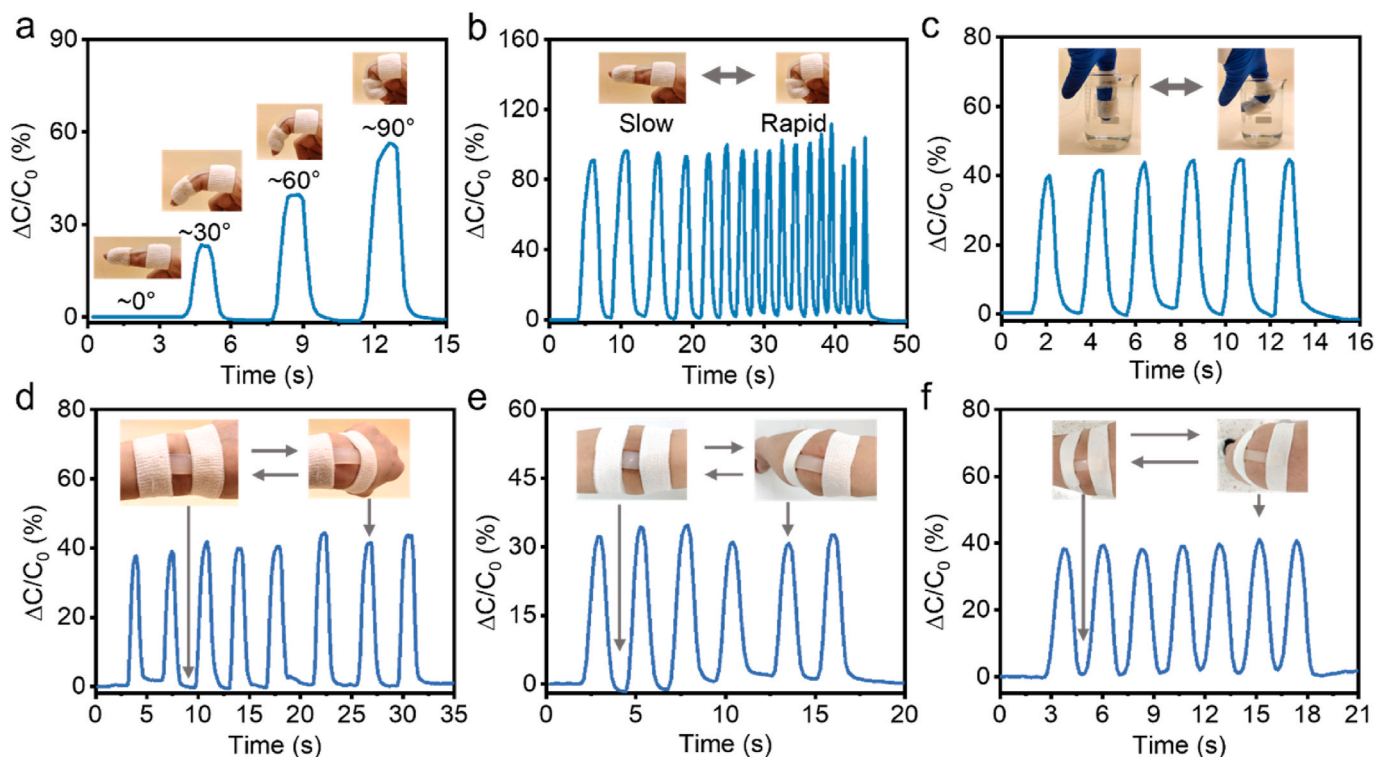


**Fig. 4.** The demonstration of the SPGLH sensor detecting human motions. (a) Relative capacitance change of the SPGLH sensor at different bending angles of the index finger. (b) The response signals of the SPGLH sensor monitoring the index finger from slow to fast bending. (c) Detection curves of the SPGLH sensor under saline. (d–f) The signals of wrist, elbow, and knee bending.

aqueous SH solution. AAm monomer was dissolved in SH aqueous solution (the ratio of 1:3) and stirred manually at room temperature until fully dissolved. LiCl powder (16.5 wt.%), glycerin (13.8 wt.%), cross-linking agent of MBAA (0.4 wt.% of AAm) as well as PEGDA (0.42 wt.% of AAm), and photoinitiator of Irgacure 2959 (0.2 wt.%) are then added in sequence and manually stirred at room temperature. The mixed solution was set for 24 h to remove air bubbles at room temperature.

#### 4.3. The fabrication of the SPGLH sensor

The surface of VHB with the size of 50 mm (length)  $\times$  15 mm (width)  $\times$  500  $\mu$ m (thickness) was treated with 10 wt.% benzophenone solution through the same method from previous work [38]. The Pt wire with a diameter of 200  $\mu$ m was attached to the side of VHB. The mold of PET film (about 200  $\mu$ m thick) with patterns was cut by a laser cutting machine (HORATEK VLS3.50) and placed on the surface of VHB. SPGLH pro-gel solution was poured into the mold of the PET film and then covered with sheet glass on top. After ultraviolet irradiation for 15 min, removing the PET film and glass, SPGLH was successfully photocured on the VHB surface. Subsequently, the surface of Ecoflex (the size of 50 mm (length)  $\times$  15 mm (width)) was treated with oxygen plasma (Plasma cleaner, ION 40). The hybrid of SPGLH and VHB was encapsulated with Ecoflex using commercial glue and set aside for about 24 h until the glue was fully cured. The above steps were repeated to integrate the Pt wire, hydrogel, and encapsulation in sequence on the other side of VHB.

The preparation process for the SPH sensor was the same as for the SPGLH sensor.

#### 4.4. Characterization

The cross-sectional morphology of SPGLH hydrogel and VHB was characterized by CCD industrial microscope (48 MP, Asaint). FTIR spectra and Raman spectra are obtained by using Fourier transform infrared spectrometer (VERTEX80v, Bruker) and Confocal micro-Raman

spectrometer (LABRAM HR EVOLUTION, HORIBA JY), respectively.

#### 4.5. Mechanical test

The mechanical performance of the hydrogels was performed by a tensile machine (YL-S71, Yuelian). To measure the interfacial toughness, adhered sample of SPGLH and VHB was prepared and subjected to the 90° peeling test. The peeling speed was 20 mm/min. The SPGLH was adhered to a PET sheet by using cyanoacrylate glue (Loctite 406, Henkel) as a stiff backing. For tensile tests, samples of hydrogels with the same size of 60 mm (length)  $\times$  10 mm (width) were photocured on the surface of VHB and were stretched at 20 mm/min until hydrogels broke.

#### 4.6. Water retention test

The hydrogels with the same size of 20 mm (length)  $\times$  6 mm (width)  $\times$  1 mm (thickness) were photocured on the surface of VHB and placed in the environment with temperature of 25 °C and relative humidity of 10% RH. The weight of the hydrogels was recorded at intervals.

#### 4.7. Electrical properties test

The conductivity of SPH, SPGH, SPLH, and SPGLH (25 mm<sup>2</sup> in cross-sectional area, and 2.5 mm in length) was tested by an electrochemical workstation (Autolab PGSTAT302 N, Metrohm). The calculation formula of conductivity was defined as Eq. (1):

$$\sigma = \frac{L}{R \times S} \quad (1)$$

where L, R, and S were the length, resistance, and area of hydrogels, respectively.

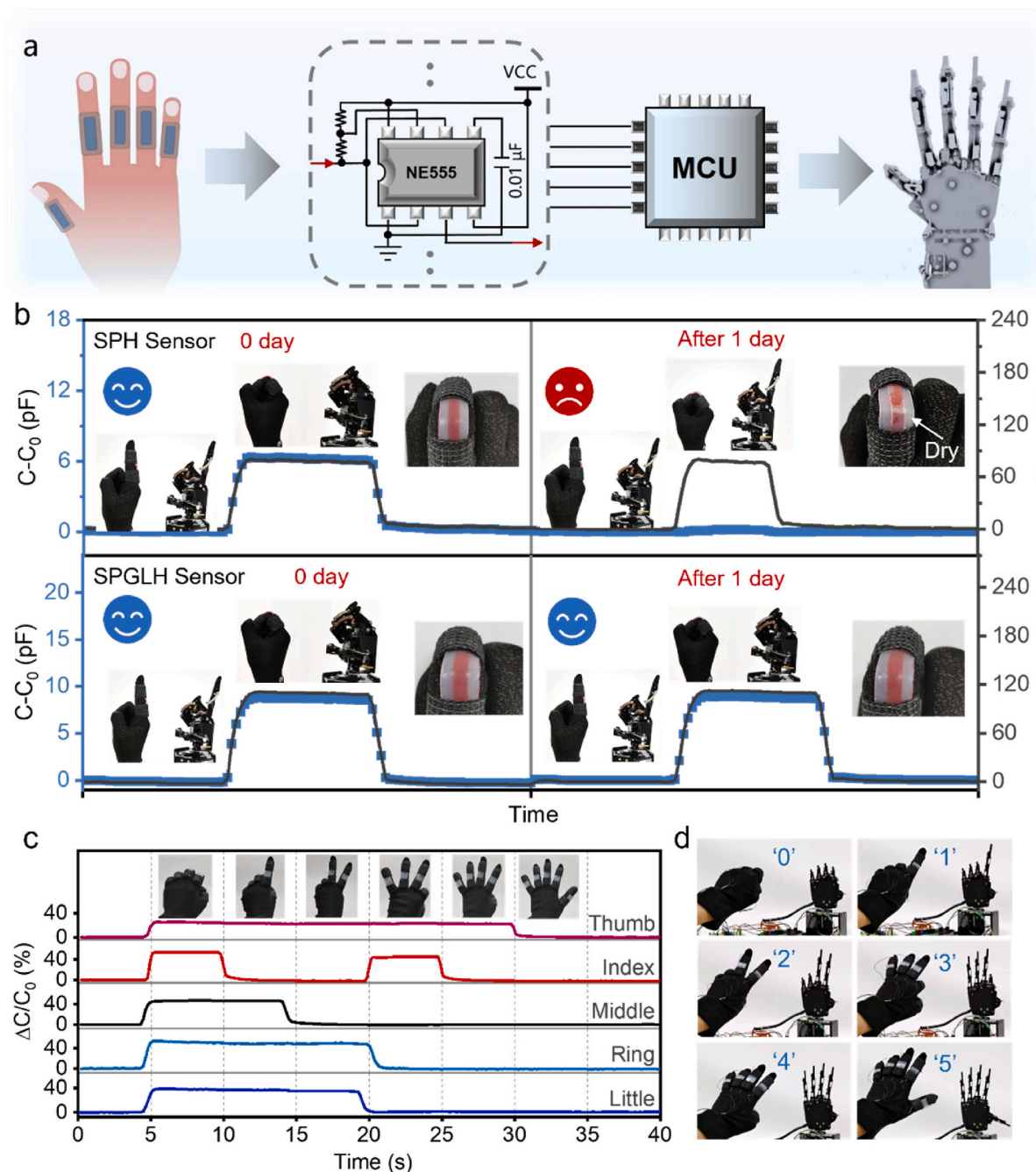


**Fig. 5.** The application of human-machine interaction in real-time. (a) Schematic diagram of the human-machine interaction system. (b) Response signals and photographs of the SPH sensor and the SPGLH sensor for controlling the robot before and after 1 day. (c) Real-time signals for each finger in different gestures. (d) Demonstration of the machine hand controlled by human hand making gestures.

#### 4.8. Sensing performance of sensors

To test the sensing performances, the sensor was fixed between the linear motor (LinMot) and the platform by adhesive tapes or homemade clamps, and the linear motor stretched the device to a certain strain. Meanwhile, capacitance signals of sensors were collected and recorded by an LCR meter (E4980A, Agilent) at a testing frequency of 1 kHz. To test humidity stability, the SPGLH sensor was placed into a constant temperature and humidity test chamber (Aerospace Zhida Test Equipment Co., Ltd. Y-HD-150 L) for over 3 h and was measured by the linear motor and an LCR meter. To test mechanical stability, the SPH sensor and the SPGLH sensor were applied at dynamic loading of 50% strain by the linear motor at 100 mm/min, respectively.

#### Author statement

Jiaoya Huang: Conceptualization, Validation, Software, Writing-Original draft preparation. Runhui Zhou: Data Curation. Ziyu Chen: Visualization. Yushu Wang and Zemin Li: Investigation. Xiaoming Mo: Supervision. Naiwei Gao: Writing-Reviewing and Editing. Jiang He: Conceptualization, Methodology, Supervision. Caofeng Pan: Writing-Reviewing and Editing, Resources, Project administration, Funding acquisition.

#### Declaration of competing interest

The authors declare that they have no known competing financial

interests or personal relationships that could have appeared to influence the work reported in this paper.

## Data availability

Data will be made available on request.

## Acknowledgments

The authors thank the support of National Natural Science Foundation of China (No. 52125205, 52250398, U20A20166, 52192614 and 52003101), National key R&D program of China (2021YFB3200302 and 2021YFB3200304) and the Fundamental Research Funds for the Central Universities.

## Appendix A. Supplementary data

Supplementary data to this article can be found online at <https://doi.org/10.1016/j.mtphys.2023.101123>.

## References

- C. Wang, C. Pan, Z. Wang, Electronic skin for closed-loop systems, *ACS Nano* 13 (2019) 12287–12293, <https://doi.org/10.1021/acsnano.9b06576>.
- Y. Peng, J. Lu, D. Peng, W. Ma, F. Li, Q. Chen, X. Wang, J. Sun, H. Liu, C. Pan, Dynamically modulated GaN whispering gallery lasing mode for strain sensor, *Adv. Funct. Mater.* 29 (2019) 1905051, <https://doi.org/10.1002/adfm.201905051>.
- D. Zhang, X. Meng, W. Hou, W. Hu, J. Mo, T. Yang, W. Zhang, Q. Fan, L. Liu, B. Jiang, L. Chu, M. Li, Solid polymer electrolytes: ion conduction mechanisms and enhancement strategies, *Nano Res. Energy* (2023): e9120050, <https://doi.org/10.26599/NRE.2023.9120050>.
- G. Liang, X. Li, Y. Wang, S. Yang, Z. Huang, Q. Yang, D. Wang, B. Dong, M. Zhu, C. Zhi, Building durable aqueous K-ion capacitors based on MXene family, *Nano Res. Energy* 1 (2022): e9120002, <https://doi.org/10.26599/NRE.2022.9120002>.
- Y. Li, Y. Liu, S.R.A. Bhuiyan, Y. Zhu, S. Yao, Printed strain sensors for on-skin electronics, *Small Struct.* 3 (2021): 2100131, <https://doi.org/10.1002/ssr.202100131>.
- R. Wei, J. He, S. Ge, H. Liu, X. Ma, J. Tao, X. Cui, X. Mo, Z. Li, C. Wang, C. Pan, Self-powered all-optical tactile sensing platform for user-interactive interface, *Adv. Mater. Technol.* 8 (2022): 2200757, <https://doi.org/10.1002/admt.202200757>.
- C. Wang, J. Zhao, C. Ma, J. Sun, L. Tian, X. Li, F. Li, X. Han, C. Liu, C. Shen, L. Dong, J. Yang, C. Pan, Detection of non-joint areas tiny strain and anti-interference voice recognition by micro-cracked metal thin film, *Nano Energy* 34 (2017) 578–585, <https://doi.org/10.1016/j.nanoen.2017.02.050>.
- J. Ren, W. Zhang, Y. Wang, Y. Wang, J. Zhou, L. Dai, M. Xu, A graphene rheostat for highly durable and stretchable strain sensor, *InfoMat* 1 (2019) 396–406, <https://doi.org/10.1002/inf2.12030>.
- Y. Liu, R. Bao, J. Tao, J. Li, M. Dong, C. Pan, Recent progress in tactile sensors and their applications in intelligent systems, *Sci. Bull.* 65 (2020) 70–88, <https://doi.org/10.1016/j.scib.2019.10.021>.
- J. He, R. Zhou, Y. Zhang, W. Gao, T. Chen, W. Mai, C. Pan, Strain-insensitive self-powered tactile sensor arrays based on intrinsically stretchable and patternable ultrathin conformal wrinkled graphene-elastomer composite, *Adv. Funct. Mater.* 32 (2021), <https://doi.org/10.1002/adfm.202107281>.
- Y. Lu, X. Qu, W. Zhao, Y. Ren, W. Si, W. Wang, Q. Wang, W. Huang, X. Dong, Highly stretchable, elastic, and sensitive MXene-based hydrogel for flexible strain and pressure sensors, *Research* (2020): 2038560, <https://doi.org/10.34133/2020/2038560>, 2020.
- J. Li, R. Bao, J. Tao, M. Dong, Y. Zhang, S. Fu, D. Peng, C. Pan, Visually aided tactile enhancement system based on ultrathin highly sensitive crack-based strain sensors, *Appl. Phys. Rev.* 7 (2020): 011404, <https://doi.org/10.1063/1.5129468>.
- Q. Hua, J. Sun, H. Liu, R. Bao, R. Yu, J. Zhai, C. Pan, Z.L. Wang, Skin-inspired highly stretchable and conformable matrix networks for multifunctional sensing, *Nat. Commun.* 9 (2018) 244–255, <https://doi.org/10.1038/s41467-017-02685-9>.
- Y. Wan, J. Tao, M. Dong, L. Zhang, Z. Peng, R. Bao, C. Pan, Flexible intelligent sensing system for plane complex strain monitoring, *Adv. Mater. Technol.* 7 (2022): 2200386, <https://doi.org/10.1002/admt.202200386>.
- J. Li, Z. Yuan, X. Han, C. Wang, Z. Huo, Q. Lu, M. Xiong, X. Ma, W. Gao, C. Pan, Biologically inspired stretchable, multifunctional, and 3D electronic skin by strain visualization and triboelectric pressure sensing, *Small Sci.* 2 (2021): 2100083, <https://doi.org/10.1002/smssc.202100083>.
- G. Li, C. Li, G. Li, D. Yu, Z. Song, H. Wang, X. Liu, H. Liu, W. Liu, Development of conductive hydrogels for fabricating flexible strain sensors, *Small* 18 (2022): e2101518, <https://doi.org/10.1002/smll.202101518>.
- V.K. Rao, N. Shauloff, X. Sui, H.D. Wagner, R. Jelinek, Polydiacetylene hydrogel self-healing capacitive strain sensor, *J. Mater. Chem. C* 8 (2020) 6034–6041, <https://doi.org/10.1039/D0TC00576B>.
- J.Y. Sun, C. Keplinger, G.M. Whitesides, Z. Suo, Ionic skin, *Adv. Mater.* 26 (2014) 7608–7614, <https://doi.org/10.1002/adma.201403441>.
- J. Zhang, Q. Zhang, X. Liu, S. Xia, Y. Gao, G. Gao, Flexible and wearable strain sensors based on conductive hydrogels, *J. Polym. Sci.* 60 (2022) 2663–2678, <https://doi.org/10.1002/pol.20210935>.
- G. Ge, W. Yuan, W. Zhao, Y. Lu, Y. Zhang, W. Wang, P. Chen, W. Huang, W. Si, X. Dong, Highly stretchable and autonomously healable epidermal sensor based on multi-functional hydrogel frameworks, *J. Mater. Chem. A* 7 (2019) 5949–5956, <https://doi.org/10.1039/C9TA00641A>.
- H. Liu, Y. Wang, Z. Shi, D. Tan, X. Yang, L. Xiong, G. Li, Y. Lei, L. Xue, Fast self-assembly of photonic crystal hydrogel for wearable strain and temperature sensor, *Small Methods* 6 (2022): 2200461, <https://doi.org/10.1002/smt.202200461>.
- J. Zhang, L. Wan, Y. Gao, X. Fang, T. Lu, L. Pan, F. Xuan, Highly stretchable and self-healable MXene/polyvinyl alcohol hydrogel electrode for wearable capacitive electronic skin, *Adv. Electron. Mater.* 5 (2019): 1900285, <https://doi.org/10.1002/aelm.201900285>.
- F. Mo, Y. Huang, Q. Li, Z. Wang, R. Jiang, W. Gai, C. Zhi, A highly stable and durable capacitive strain sensor based on dynamically super-tough hydro/organogels, *Adv. Funct. Mater.* 31 (2021): 2010830, <https://doi.org/10.1002/adfm.202010830>.
- X. Dai, Y. Long, B. Jiang, W. Guo, W. Sha, J. Wang, Z. Cong, J. Chen, B. Wang, W. Hu, Ultra-antifreeze, ultra-stretchable, transparent, and conductive hydrogel for multi-functional flexible electronics as strain sensor and triboelectric nanogenerator, *Nano Res.* 15 (2022) 5461–5468, <https://doi.org/10.1007/s12274-022-4153-5>.
- K.H. Lee, Y.Z. Zhang, H. Kim, Y. Lei, S. Hong, S. Wustoni, A. Hama, S. Inal, H. N. Alshareef, Muscle fatigue sensor based on Ti(3) C(2) T(x) MXene hydrogel, *Small Methods* 5 (2021): e2100819, <https://doi.org/10.1002/smt.202100819>.
- R. Miyakoshi, S. Hayashi, M. Terakawa, Direct patterning of conductive structures on hydrogels by laser-based graphitization for supercapacitor fabrication, *Adv. Electron. Mater.* (2023): 2201277, <https://doi.org/10.1002/aelm.202201277>.
- C. Wang, Y. Liu, X. Qu, B. Shi, Q. Zheng, X. Lin, S. Chao, C. Wang, J. Zhou, Y. Sun, G. Mao, Z. Li, Ultra-stretchable and fast self-healing ionic hydrogel in cryogenic environments for artificial nerve fiber, *Adv. Mater.* 34 (2022): e2105416, <https://doi.org/10.1002/adma.202105416>.
- W. Peng, X. Pan, X. Liu, Y. Gao, T. Lu, J. Li, M. Xu, L. Pan, A moisture self-regenerative, ultra-low temperature anti-freezing and self-adhesive polyvinyl alcohol/polyacrylamide/CaCl(2)/MXene ionotronics hydrogel for bionic skin strain sensor, *J. Colloid Interface Sci.* 634 (2023) 782–792, <https://doi.org/10.1016/j.jcis.2022.12.101>.
- H. Sun, Y. Zhao, S. Jiao, C. Wang, Y. Jia, K. Dai, G. Zheng, C. Liu, P. Wan, C. Shen, Environment tolerant conductive nanocomposite organohydrogels as flexible strain sensors and power sources for sustainable electronics, *Adv. Funct. Mater.* 31 (2021): 2101696, <https://doi.org/10.1002/adfm.202101696>.
- P. He, J. Wu, X. Pan, L. Chen, K. Liu, H. Gao, H. Wu, S. Cao, L. Huang, Y. Ni, Anti-freezing and moisturizing conductive hydrogels for strain sensing and moist-electric generation applications, *J. Mater. Chem. A* 8 (2020) 3109–3118, <https://doi.org/10.1039/c9ta12940e>.
- X. Sui, H. Guo, C. Cai, Q. Li, C. Wen, X. Zhang, X. Wang, J. Yang, L. Zhang, Ionic conductive hydrogels with long-lasting antifreezing, water retention and self-regeneration abilities, *Chem. Eng. J.* 419 (2021): 129478, <https://doi.org/10.1016/j.cej.2021.129478>.
- H. Huang, L. Han, X. Fu, Y. Wang, Z. Yang, L. Pan, M. Xu, Multiple stimuli responsive and identifiable zwitterionic ionic conductive hydrogel for bionic electronic skin, *Adv. Electron. Mater.* 6 (2020): 2000239, <https://doi.org/10.1002/aelm.202000239>.
- C. Yang, Z. Suo, Hydrogel ionotronics, *Nat. Rev. Mater.* 3 (2018) 125–142, <https://doi.org/10.1038/s41578-018-0018-7>.
- M. Guo, J. Yan, X. Yang, J. Lai, P. An, Y. Wu, Z. Li, W. Lei, A.T. Smith, L. Sun, A transparent glycerol-hydrogel with stimuli-responsive actuation induced unexpectedly at subzero temperatures, *J. Mater. Chem. A* 9 (2021) 7935–7945, <https://doi.org/10.1039/d1ta00112d>.
- Y. Bai, B. Chen, F. Xiang, J. Zhou, H. Wang, Z. Suo, Transparent hydrogel with enhanced water retention capacity by introducing highly hydratable salt, *Appl. Phys. Lett.* 105 (2014): 151903, <https://doi.org/10.1063/1.4898189>.
- G. Zhang, S. Chen, Z. Peng, W. Shi, Z. Liu, H. Shi, K. Luo, G. Wei, H. Mo, B. Li, L. Liu, Topologically enhanced dual-network hydrogels with rapid recovery for low-hysteresis, self-adhesive epidemic electronics, *ACS Appl. Mater. Interfaces* 13 (2021) 12531–12540, <https://doi.org/10.1021/acscami.1c00819>.
- Z. Wang, L. Chen, Y. Chen, P. Liu, H. Duan, P. Cheng, 3D printed ultrastretchable, hyper-antifreezing conductive hydrogel for sensitive motion and electrophysiological signal monitoring, *Research* (2020): 1426078, <https://doi.org/10.34133/2020/1426078>, 2020.
- H. Yuk, T. Zhang, G.A. Parada, X. Liu, X. Zhao, Skin-inspired hydrogel-elastomer hybrids with robust interfaces and functional microstructures, *Nat. Commun.* 7 (2016): 12028, <https://doi.org/10.1038/ncomms12028>.
- H. Jin, M.O.G. Nayeem, S. Lee, N. Matsuhisa, D. Inoue, T. Yokota, D. Hashizume, T. Someya, Highly durable nanofiber-reinforced elastic conductors for skin-tight electronic textiles, *ACS Nano* 13 (2019) 7905–7912, <https://doi.org/10.1021/acsnano.9b02297>.
- R. Nur, N. Matsuhisa, Z. Jiang, M.O.G. Nayeem, T. Yokota, T. Someya, A highly sensitive capacitive-type strain sensor using wrinkled ultrathin gold films, *Nano Lett.* 18 (2018) 5610–5617, <https://doi.org/10.1021/acs.nanolett.8b02088>.
- J.C. Yang, J. Mun, S.Y. Kwon, S. Park, Z. Bao, S. Park, Electronic skin: recent progress and future prospects for skin-attachable devices for health monitoring, robotics, and prosthetics, *Adv. Mater.* 31 (2019): e1904765, <https://doi.org/10.1002/adma.201904765>.

- [42] J. Qin, L.J. Yin, Y.N. Hao, S.L. Zhong, D.L. Zhang, K. Bi, Y.X. Zhang, Y. Zhao, Z. M. Dang, Flexible and stretchable capacitive sensors with different microstructures, *Adv. Mater.* 33 (2021): e2008267, <https://doi.org/10.1002/adma.202008267>.
- [43] J. Yuan, Y. Zhang, G. Li, S. Liu, R. Zhu, Printable and stretchable conductive elastomers for monitoring dynamic strain with high fidelity, *Adv. Funct. Mater.* 32 (2022), <https://doi.org/10.1002/adfm.202204878>.
- [44] M. Lin, Z. Zheng, L. Yang, M. Luo, L. Fu, B. Lin, C. Xu, A high-performance, sensitive, wearable multifunctional sensor based on rubber/CNT for human motion and skin temperature detection, *Adv. Mater.* 34 (2022): e2107309, <https://doi.org/10.1002/adma.202107309>.